IEEE Access
Multidisciplinary : Rapid Review : Open Access Journal

Received April 15, 2021, accepted May 6, 2021, date of publication May 10, 2021, date of current version June 25, 2021.

Digital Object Identifier 10.1109/ACCESS.2021.3078764

Study on the Appropriate Measurement Spacing for EMF Installation Compliance Assessments of a 3.5 GHz 5G Base Station

YOUNG SEUNG LEE[1], (Member, IEEE), SANG BONG JEON[1], AE-KYOUNG LEE[1], KIHWEA KIM[2], JEONG-KI PACK[3], AND HYUNG-DO CHOI[1]

[1]Radio and Satellite Research Division, Electronics and Telecommunications Research Institute, Daejeon 34129, South Korea
[2]Radio Environment Safety Division, National Radio Research Agency, Naju 58323, South Korea
[3]Department of Radio and Information Communications Engineering, Chungnam National University, Daejeon 34134, South Korea

Corresponding author: Young Seung Lee (lys009@etri.re.kr)

This work was supported by the MSIT/IITP through the ICT Research and Development Program (A Study on Public Health and Safety in a Complex EMF Environment) under Grant 2019-0-00102.

ABSTRACT The number of fifth generation (5G) base stations (BSs) installed for commercial services continues to increase in South Korea since the first 5G rollout of the 3.5 GHz band in 2019. However, this will cause a rapid increase in the cost and effort required for an electromagnetic field (EMF) installation compliance measurements of a 5G BS. This paper studies an appropriate measurement spacing for EMF installation compliance assessments of a 3.5 GHz 5G BS. Ray-tracing simulations based on the ray frustum technique are performed for three installation scenarios according to the accessibility categories provided in the International Telecommunication Union-T K.52 recommendation to observe the power density exposure trends. An interference analysis using the two-ray propagation model indicates that the spacing of 1 m can be suitable for the installation compliance of a 5G BS above 3 GHz. In addition, it was found that this spacing could be also applied up to the higher frequency of 7.125 GHz, the upper limit of Frequency Range 1 defined in the 3rd Generation Partnership Project specification. Measurements based on two different 5G signal extrapolations using the Synchronization Signal Block were conducted to validate the spacing of 1 m for a 3.5 GHz 5G BS established by simulation studies.

INDEX TERMS Base station, 5G, 3.5 GHz, measurement spacing, interference, installation compliance.

I. INTRODUCTION

The fifth generation (5G) communication system is currently attracting significant attention worldwide owing to its enhanced capabilities of supporting various applications [1]. Since the first commercial launch of the 5G network at 3.5 GHz in April of 2019 [2], [3], the number of subscribers to 5G services has reached approximately 7 million in South Korea [4].

However, this has resulted in a proliferation of extra base stations (BSs) necessary for providing higher capacity and faster data transmission speeds required for 5G services. Although the number of 5G BSs currently installed nationwide in South Korea exceeds approximately 100,000, this is still far fewer than those for the fourth generation Long Term Evolution service [5], [6] and there is still a rapid increase in the 5G BS density for an actual cellular network due to the larger propagation losses at the higher frequency bands introduced in 5G communications.

Public concerns related to the 5G electromagnetic field (EMF) exposures, however, can have a considerable impact on the industrial and economic issues about the 5G service [7]. Compliance with the current exposure limit can also inhibit and hinder installations of the high performance 5G network [8]. Recently, the uplink and downlink power were measured and the exposure levels were also evaluated in the 5G network in Seoul, the capital city of South Korea [6]. The heatlth effects due to the 5G millimeter-wave (MMW) exposures is well discussed in a systematic review [9] as well. Many studies have been also recently available on the actual exposure measurements of a 5G BS for EMF compliance mainly based on the extrapolation technique by using the 'always-on' Synchronization Signal Block (SSB) signal [10]–[13]. However, the large number of 5G BSs will result

The associate editor coordinating the review of this manuscript and approving it for publication was Guido Valerio.

in an increase in the measurement cost and effort required for BS compliance assessments as a consequence.

The current BS standard of the International Electrotechnical Commission [14] requires moving the probe slowly inside the accessible area to find the maximum exposure level and distance for installation compliance measurements. This procedure, however, can cause more ambiguity in measurement results for assessments due to the unspecified movement speed of a measurement probe as well as the dynamic behavior of propagation environments. In addition, the new technologies employed for 5G communications, e.g., the beamforming technique [15] and flexible numerology [11]–[13] should make it more difficult to conduct EMF measurements for a 5G BS compliance assessment. Hence, an appropriate measurement spacing Δ adequate for the maximum power density (PD) can be very useful for 5G BS installation compliances. Promising candidates to treat this problem are the spacing of $\Delta \leq 50$ cm for frequencies of above 3 GHz and $\Delta \leq 1$ m for frequencies of below 3 GHz, specified in the European standard [16]. These spacings have been also adopted for the EMF installation compliance of BSs in South Korea [17], as defined in [18].

The remainder of this paper is organized as follows: Section II describes the ray-tracing approaches, simulation scenarios and measurement methods employed to establish the appropriate measurement spacing. Section III proposes the spacing based on the analyses on various exposure trends from a 5G BS. Finally, some concluding remarks are given in Section IV.

II. APPROACH AND METHOD

This section presents the exposure assessment method of a 3.5 GHz 5G BS to establish an appropriate measurement spacing. The proposed approach consists of two stages: simulations and measurements.

A. SIMULATION

1) RAY-TRACING ANALYSIS

The ray-tracing method has been used for various applications over wide frequency ranges from gigahertz [19] to MMW [20] bands, even for terahertz applications [21]. Hence, the ray-tracing software developed by the authors for a 5G MMW BS compliance [22] is employed for simulations throughout the paper. This software is based on the ray frustum algorithm [23] for a computational acceleration, which originates from computer graphics and visualization [24], [25]. The ray-frustum-based tracing has also been considered to predict the propagation characteristics of the 5G MMW channel [26], [27] and the orbital angular momentum waves [28] in efficient way.

2) SIMULATION SCENARIOS

Various simulations are conducted for three different installation scenarios based on the accessibility categories defined in the International Telecommunication Union (ITU)-T

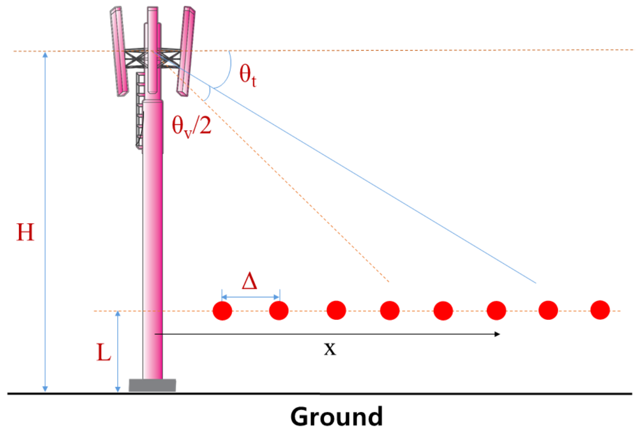

FIGURE 1. Schematic geometry of Scenario 1 with few significant reflecting structures near a BS.

K.52 recommendation [29] for estimation of the maximum exposure from a BS. These scenarios have been adopted in [29] to incorporate most of the practical installation environments and locations of outdoor 3.5 GHz 5G BSs, which are now very similar to those of the previous generations. In addition, higher-order reflections due to propagation mechanisms in a complex urban environment (e.g., a street caynon etc) have not a strong influence on the major exposure trend governed by the two-ray propagation [30]. Hence, these three scenarios [29] can be useful to investigate the dominant exposure behavior of a 3.5 GHz 5G BS near the maximum distance in many practical situations.

Scenario 1, schematically shown in Figure 1, corresponds to an installation site with few reflecting structures (e.g., buildings and houses) that significantly affect the electromagnetic field strength emitted from a BS antenna, similar to the accessibility category 1 described in [29]. Hence, the wave propagation and attenuation depend primarily on the ground reflection in this case. Here, H is the BS installation height from the ground level, L is the observation (computation or measurement) height occupied by a human body, Δ is the measurement spacing between two neighboring points, θ_t is the downtilt angle of a BS (mechanical and electrical), θ_v is the elevation (vertical) half-power beamwidth (HPBW) of a BS antenna, and x denotes the horizontal distance from the BS, respectively. Because the observation height L of 1.5 m has been currently adopted as the standard for conducting general exposure measurements for a BS installation compliance [14], [18], [31], all simulations are also performed based on a height of $L = 1.5$ m.

In a similar manner, Scenarios 2 and 3, depicted in Figure 2, describe the installation environments with a significant reflecting structure (e.g., building and house) causing considerable variation in the direct incident field emitted from a BS. Here, D is the distance between a BS and a building, and the building height H' is approximately similar to and relatively smaller than the BS installation height H in the case of Scenarios 2 and 3, respectively, as in the accessibility categories 2 and 3 of [29]. Note that the BS installation height

TABLE 1. BS specifications adopted for the simulations.

Parameter	Value
Frequency	3.65 GHz
Input power	50 dBm
Maximum gain	21.5 dBi
Elevation HPBW (θ_v)	10°
Azimuth HPBW	90°
Downtilt angle (θ_t)	15°
Polarization	Vertical
Side lobe level	-30 dB

H should be defined from the ground level regardless of the installation environment of the BS. The observation height L should be above the top of the building (e.g., a rooftop) when a horizontal observation path encounters a building surface, which is also clearly incorporated in the estimation formula of [29].

The single continuous wave at a frequency of 3.65 GHz, one of the carrier frequencies used in current 5G commercial networks in South Korea, is assumed for analysis. Table 1 lists the BS specifications adopted for the simulations in accordance with a commercial 5G BS currently installed for the 5G network used in South Korea as discussed below (see Section II-B). Note that the input power and the maximum gain given in Table 1 indicates the maximum power transmission from a BS, i.e., the full traffic case considered for a BS installation compliance assessment based on the extrapolation approach [10]–[13]. This input power of 50 dBm is also the same as one used in simulation [32] and similar to one used in measurement study of 53 dBm [33], respectively. A constant side lobe level of -30 dB stems from the antenna model defined in the 3rd Generation Partnership Project (3GPP) channel report [34]. The dielectric constant ε_r and the conductivity σ of the building and ground surface are assumed as $\varepsilon_r = 6.09$, $\sigma = 0.0156$, and $\varepsilon_r = 5.6$, $\sigma = 0.01$, respectively [35]. A numerical validation of the ray-frustum-based software [22] is performed by comparing the results to those obtained from a commercially available ray-tracing software of Wireless InSite using the shooting and bouncing ray method.

It should be noted here that although the installation geometry is modeled only on the elevation plane under all three scenarios shown in Figures 1 and 2, this simplification has been a conventional approach for a BS compliance assessment [29], [36], [37] because the maximum exposure mostly occurs along the direction of the maximum radiation at the azimuth plane.

B. MEASUREMENT

Measurements of a 3.5 GHz BS are also carried out to validate the spacing Δ determined from the simulations as discussed in Section II-A. Actual measurements are conducted at a commercial site of a 3.5 GHz 5G BS located in Daejeon, South Korea.

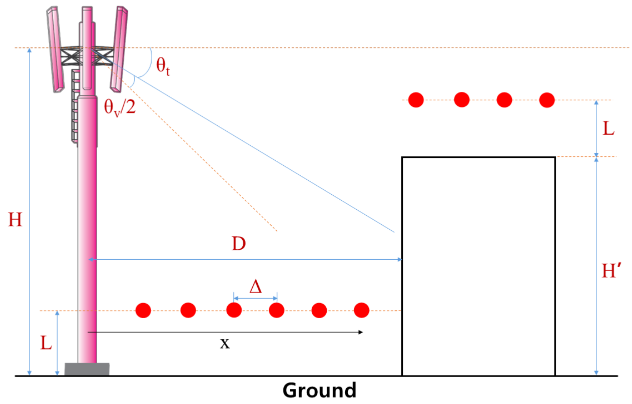

(a)

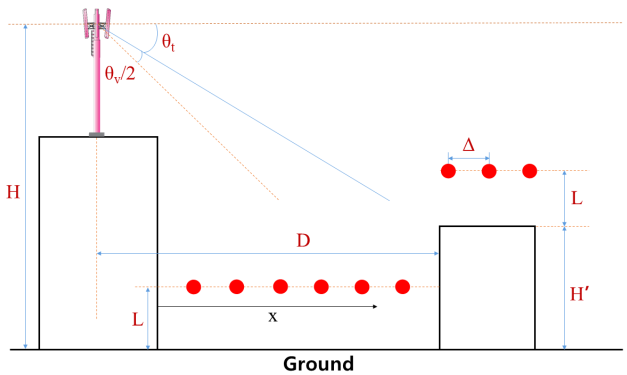

(b)

FIGURE 2. Schematic geometry of Scenarios 2 and 3 with a significant reflecting structure of height H' near a BS; (a) Scenario 2 ($H' \simeq H$); (b) Scenario 3 ($H' \ll H$).

The specifications of the BS are listed in Table 1 (see Section II-A2). The geometry used for the measurements is the same as that shown in Figure 2b with dimensions of $H = 37$ m, $H' = 22$ m, and $D = 53$ m. The measurement points at $L = 1.5$ m on the ground and rooftop, represented by the red-filled circles, can also be seen.

The methods by means of the New Radio (NR) signal extrapolation using the SSB are employed for measurements [14]. Two different methods are based on different instrument functions: a dedicated NR decoder (hereafter referred to as "Decoding") and a spectrum analyzer (SA) in zero span mode (hereafter referred to as "Zero Span"). An Anritsu MS2090A Spectrum Analyzer and a Rohde & Schwarz FPH Spectrum Rider are used for the Decoding and the Zero Span methods, respectively. Figure 3 shows photographs of a 3.5 GHz BS at each measurement site (i.e., the ground and rooftop) with two different probes corresponding to two NR measurement methods. All measurements are performed at $L = 1.5$ m in accordance with the standard height [14], [18], [31], as discussed in Section II-A, based on the spacing of $\Delta = 50$ cm as mentioned in Section I above. These two measurement results are scaled up based on the average value of simulations carried out under the maximum power transmission, and overall exposure trends are compared to each other for validation as discussed below.

(a) (b)

FIGURE 3. Photographs of the measurements of a 3.5 GHz BS located in Daejeon, South Korea; (a) at the rooftop with a probe for the Decoding method; (b) at the ground with a probe for the Zero Span method.

The Decoding method measures the electric field strength per resource element (RE) of the SSB and then determines the actual exposure level by applying the extrapolation factor. A set of parameters with the center frequency of 3650 MHz, the SSB offset of -41.22 MHz, the subcarrier spacing of 30 kHz, and the channel bandwidth of 100 MHz are used for actual measurements. The extrapolated maximum electric field strength, $E_{\max}$, is evaluated as follows:

$$\begin{aligned} E_{\max} &= E_{SSB} \times \sqrt{F_{extSSB}} \\ &= E_{SSB} \times \sqrt{F_{BW} \times F_{PR} \times F_{TDC}} \end{aligned} \tag{1}$$

where E_{SSB} is the electric field strength per RE of the SSB, F_{extSSB} is the extrapolation factor for the SSB, F_{BW} is the total number of subcarriers within the carrier bandwidth, F_{PR} is the power reduction for the actual maximum approach, and F_{TDC} is the technology duty cycle, respectively. The extrapolation factor F_{extSSB} applied to the 5G NR frame structure used by Korean mobile operators can be found in [38]. The technology duty cycle F_{TDC} of 0.743 is employed for measurements based on the 5G NR time division duplexing frame configuration of DDDSU, where D, S, U denote the downlink, special, and uplink slot, respectively [11], [12].

By contrast, with the Zero Span method, the peak electric field of the SSB is recorded using a SA in zero span mode in the time domain. The measurement setup uses the sweep time of 20 ms based on the SA resolution bandwidth of 30 kHz with the center frequency of 3608.78 MHz. An actual exposure in this case is also determined by applying the extrapolation factor, and $E_{\max}$ is defined as follows:

$$E_{\max} = E_{peak} \times \sqrt{\frac{SCS}{RBW} \times F_{BW} \times F_{PR} \times F_{TDC}} \tag{2}$$

where E_{peak} is the peak electric field strength of the SSB, SCS is the subcarrier spacing, and RBW is the resolution bandwidth of an SA, respectively.

However, it is difficult to obtain a reasonable maximum exposure level of $E_{\max}$ based on the extrapolation approach given in (1) and (2) directly since the precise information

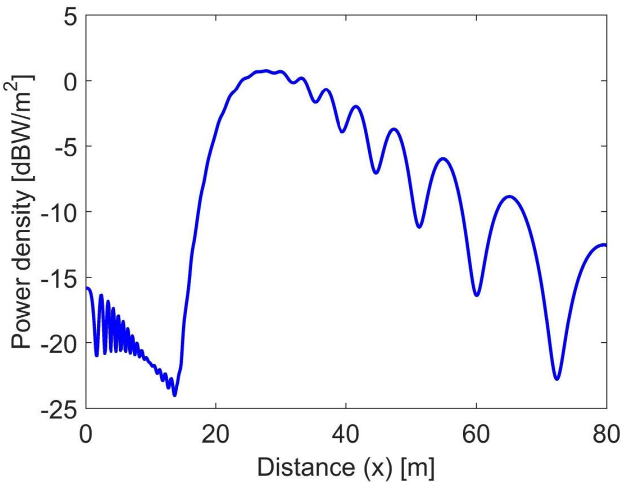

FIGURE 4. PD levels from a 3.5 GHz 5G BS in the case of Scenario 1 when $H = 10$ m and $L = 1.5$ m (exposure limit - 10 dBW/m^2).

on the 5G NR flexible frame structure must be provided for an appropriate instrument setup during compliance measurements. Hence, $E_{\max}$ is determined by means of linear scaling using the average value of ray-tracing simulations instead:

$$E_{\max} = E_{raw} \times A_{scale} \tag{3}$$

where A_{scale} is the scale factor defined as the ratio of the average value of simulations to those of measurements. Note that simulations are performed under the maximum power condition as discussed in Section II-A2. E_{raw} is the measured raw data given by E_{SSB} and E_{peak} in (1) and (2), respectively. It should be noted here that the electric field strength is used for scalings since the extrapolations of (1) and (2) are defined based on this field strength. The PD is then obtained from these measured field strengths based on the relation of $PD = \frac{E^2}{377}$ (i.e., the equivalent plane wave power density) [14], [29], [39]. Comparisons of the overall exposure behaviors are carried out to validate the appropriate spacing.

III. RESULTS AND DISCUSSION

Figure 4 shows the PD simulation results from a 5G BS for Scenario 1 (see Figure 1) versus the horizontal distance x from a BS at an observation height L of 1.5 m, as discussed in Section II-A. The installation height H is assumed to be 10 m. It can be clearly seen that the maximum PD is much smaller than the exposure limit of 10 dBW/m^2 (= 10 W/m^2) defined in the current International Commission on Non-Ionizing Radiation Protection (ICNIRP) guideline as the reference level for the whole-body exposure [40]. Note that these PDs are still well below the 10 dBW/m^2 limit even though the spatial averaging over the whole-body space is performed according to [14]. The total PD profiles analogous to estimated results in [29] can be subdivided into three regions: the side lobe (about $x \leq 18$ m), the main beam (about 18 m $\leq x \leq$ 35 m), and the interference region (about $x \geq 35$ m). Note that the "interference" is used to denote the wave interference phenomenon caused by the phase difference between two waves throughout the paper [41]. Extremely low exposure levels can be seen in the side lobe region owing to the side lobe level of a BS antenna, and the main beam region represents an increase in the PDs with increased horizontal distances from a 5G BS owing to the directional characteristics of a 5G BS antenna. The interference pattern within the farthest region, along with the propagation decays relative to the distance, is due to the constructive and destructive interference between the direct incident and reflected rays from the ground.

The simulated PD results of Scenario 1 with three different installation heights H when $L = 1.5$ m are shown in Figure 5. The exposure characteristics of the three different regions shown in Figure 4 above can also be clearly seen as expected. All PDs still do not exceed the ICNIRP limit of 10 dBW/m^2 [40]. The PD distributions are spread out with increasing installation heights owing to an increase in the wave propagation losses related to the three-dimensional distance between the BS antenna and the observation point, and the distance of the maximum exposure moves toward the interference region as the installation height H increases as a consequence. This PD behavior can be confirmed by the study in [36], which estimates the range of the maximum distance d_m (i.e., the maximum exposure occurs when $x = d_m$) based on the first-null beamwidth (FNBW) of a BS antenna as follows:

$$d_1 = \frac{H - L}{\tan \theta_t}, \qquad d_2 = \frac{H-L}{\tan\left(\theta_t + \frac{\theta_{fn}}{2}\right)},$$
$$d_2 < d_m < d_1 \tag{4}$$

where θ_{fn} is the FNBW of a BS antenna, and d_1 and d_2 are the distances corresponding to the direction of the maximum gain and the FNBW from a BS, respectively. However, it is apparent that the ranges of (4) marked by the black stars in Figure 5 are clearly an extremely rough estimate of the maximum distance d_m.

A good alternative can be the use of the vertical HPBW θ_v in (4) instead of the FNBW θ_{fn}, and the resolution capabilities of the antenna are in fact closely related to the HPBW, providing most of the propagating energy inside its coverage [42]. The ranges based on the HPBW, which are represented by the black triangles in Figure 5, actually show a significant improvement in estimations of the maximum distance d_m. Also, this estimated HPBW ranges assure the spread-out distributions of the PD levels as shown in Figure 5. Note that the figure on the right displays the PD results within this HPBW range for H = 20 m (i.e., the horizontal axis scale is expanded based on the estimated HPBW range). It can clearly be seen that the maximum distance d_m occurs inside the farthest region having an interference pattern. Unlike the other two cases, an inappropriate spacing of Δ used for compliances will not be able to capture proper samples for maximum exposure and distance, which are crucial for an EMF installation compliance assessment of a 5G BS. It should be stated that, although the overall PD profiles are in agreement with the exposure trends obtained by the spherical

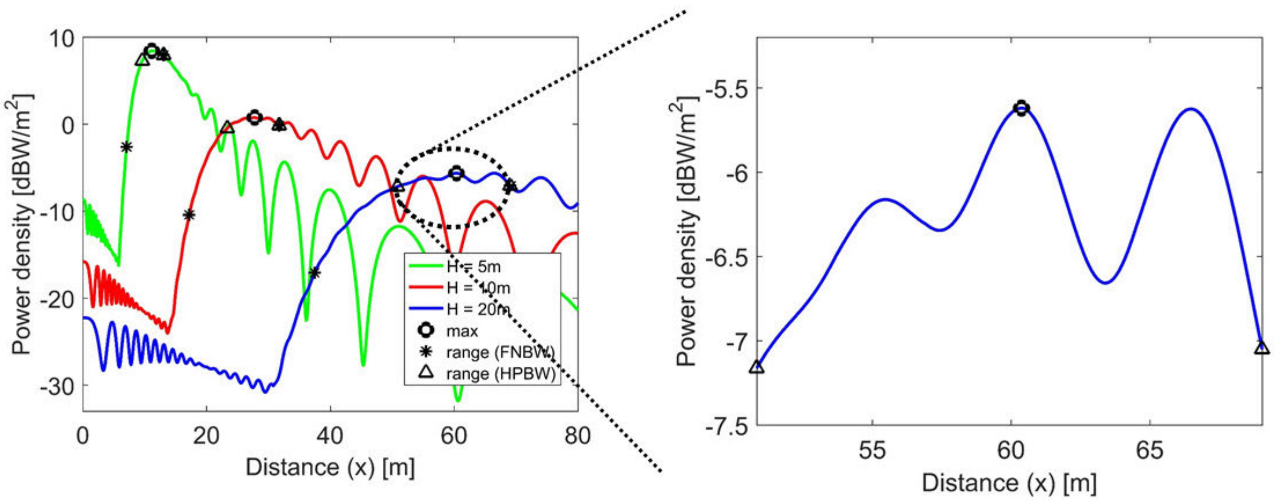

FIGURE 5. PD levels from a 3.5 GHz 5G BS with three different installation heights H for Scenario 1 when $L = 1.5$ m (exposure limit - 10 dBW/m^2).

estimation formula described in [29], those of [29] are unable to express the interference phenomena within the farthest region because of an approximation included in its derivation. Hence, an explicit analysis should be further required to determine the appropriate spacing required to reduce the measurement burden for a 5G BS.

The useful two-ray propagation model, a typical interference modeling widely used for mobile communication [43], can be employed for this purpose on the elevation geometry of Scenario 1. According to this model, the received power P_r specifying the interference owing to the ground reflection is expressed as follows:

$$P_r = \left(\frac{\lambda}{4\pi x}\right)^2 4\sin^2\left(\frac{2\pi HL}{\lambda x}\right) EIRP \cdot G_r \tag{5}$$

where λ is the wavelength, $EIRP$ is the effective isotropic radiated power of a BS, and G_r is the gain of a receiving antenna, respectively. With the relation between the effective aperture and the PD [42], the PD can be written as follows:

$$PD = \frac{EIRP}{4\pi x^2} 4\sin^2\left(\frac{2\pi HL}{\lambda x}\right) \tag{6}$$

Note that this expression is particularly suitable for the PD profile inside the interference region with an attenuation inversely proportional to x^2 and an interference from a contribution of $\sin^2\left(\frac{2\pi HL}{\lambda x}\right)$. Figure 6 illustrates this normalized PD interference pattern of $\sin^2\left(\frac{2\pi HL}{\lambda x}\right)$ for Scenario 1 within the estimated HPBW range (i.e., near the maximum distance d_m) when $H = 20$ m and $L = 1.5$ m (see Figure 5). The green circles and red crosses calculated based on a spacing of 50 cm and 1 m are also represented as discussed in Section I. Supposing that two samples are captured inside one crest of interference, it can be clearly seen that the maximum exposure can be assessed within half of the maximum interference level even under the worst situation of the shift in measurement points. However, measurements are not be able to properly detect the maximum PD and distance, or even going to record the minimum PD at worst, if one sample is missing inside one crest of interference. This indicates that at least two sample points should be provided inside one crest for reasonable compliance assessments (i.e., to suppress the maximum error within half of the interference level at worst). Actually, four to five samples can be achieved based on the data of $\Delta = 1$ m (red crosses), as shown in Figure 6a, indicating that the maximum exposure can be recorded with reasonable accuracy for a 5G BS of 3.65 GHz frequency. By contrast, more sample points can be expected to be required owing to a short interference interval with increasing frequency based on the frequency (wavelength) scaling of the electromagnetic waves [42], as clearly indicated in Figure 6b,c. Indeed, based on the spacing of $\Delta = 1$ m, two samples can be recorded for 7.125 GHz, which is the upper frequency limit of FR1 defined in the 3GPP specification [44], as indicated in Figure 6b; in contrast, only one sample is captured near the maximum distance d_m of approximately 60 m (see Figure 5) for 14 GHz, as shown in Figure 6c. Thus it is apparent that the spacing of $\Delta = 1$ m can also be applied to the FR1 up to 7.125 GHz instead of that of $\Delta = 50$ cm of a narrower one, indicating that the measurement burden for 5G BS compliances can be greatly reduced as a consequence.

In a similar manner, ray-tracing results for Scenario 2 are depicted in Figure 7. The installation parameters are assumed to be $H = 20$ m, $H' = 18$ m, and $D = 10$ m, respectively. Relatively smaller PDs can be observed on the ground path (< 10 m) because of the larger attenuation (i.e., the larger distance between a BS and an observation point). The fluctuation characteristics of the PDs near the edge of the rooftop are due to the diffractions from the edge, and the higher PDs stem from a small relative installation height from the rooftop level ($H - H'$) as can be seen in the formula of [29]. Figure 8 shows the simulation results for Scenario 3 with the same

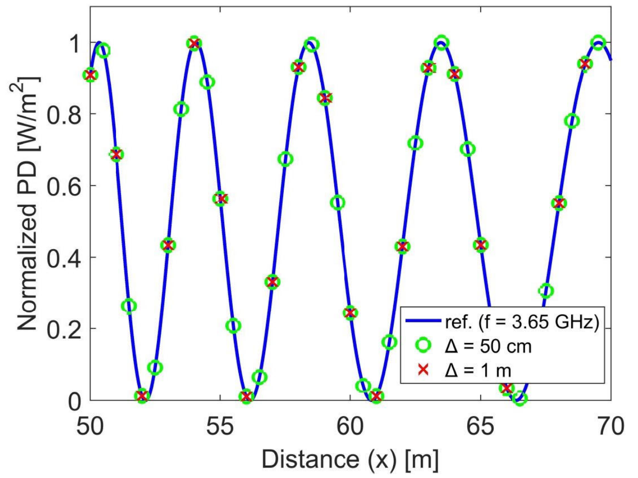

(a)

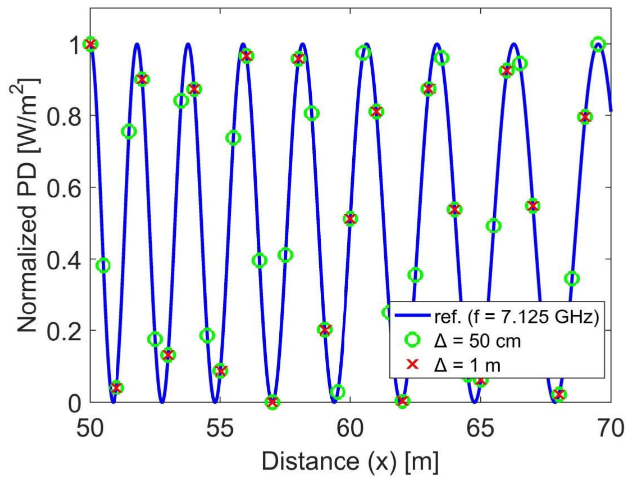

(b)

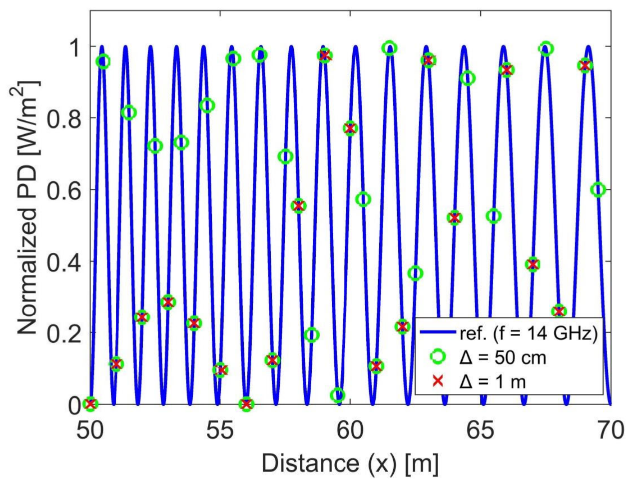

(c)

FIGURE 6. Normalized PD interference pattern near the maximum distance d_m for Scenario 1 when $H = 20$ m and $L = 1.5$ m; (a) 3.65 GHz; (b) 7.125 GHz; (c) 14 GHz.

installation parameters except for a building height of $H' = 18$ m. The expected small PD level occurs on the ground path as shown in Scenario 2 of Figure 7. Two PD curves depicted

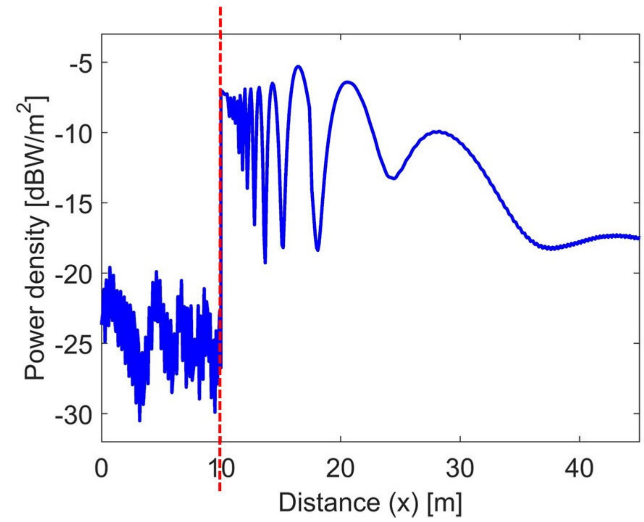

FIGURE 7. PD levels from a 3.5 GHz 5G BS for Scenario 2 when $H = 20$ m, $H' = 18$ m, $D = 10$ m, and $L = 1.5$ m (exposure limit - 10 dBW/m^2).

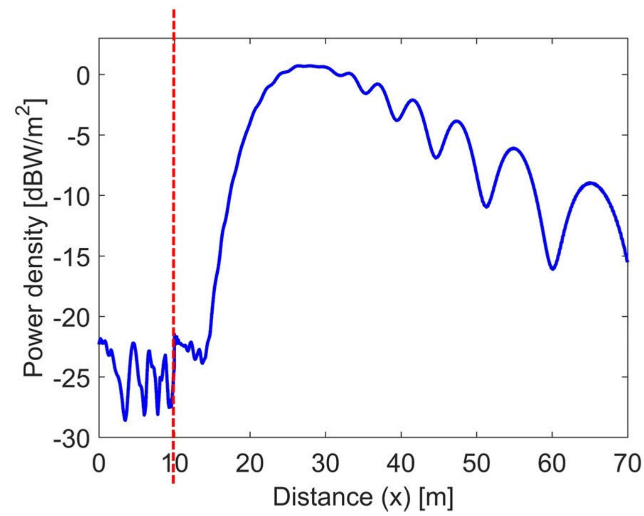

FIGURE 8. PD levels from a 3.5 GHz 5G BS for Scenario 3 when $H = 20$ m, $H' = 10$ m, $D = 10$ m, and $L = 1.5$ m (exposure limit - 10 dBW/m^2).

in Figures 7 and 8 are also below the 10 dBW/m^2 limit in [40]. It should be stated that the PD behaviors on the rooftop are in agreement with those in Figure 4 for Scenario 1 with $H = 10$ m, indicating that the PD levels emitted from a BS certainly have a strong dependence on the relative installation height of $H - H'$. As a consequence, all of the preceding discussions and the spacing of $\Delta = 1$ m determined from Scenario 1 (i.e., few reflecting structures near a BS) can also be valid for the other installation scenarios with a significant reflecting structure based on this relative height of $H - H'$.

In addition, a numerical result of the ray-frustum-based software [22] is compared with that obtained from a commercial software of Wireless InSite for validation purposes. Note that the parameters of $H = 37$ m, $H' = 22$ m, and $D = 53$ m are employed for a simulation in accordance with the dimensions of the measurement environment defined in Section II-B and the computed PD results levels on the ground

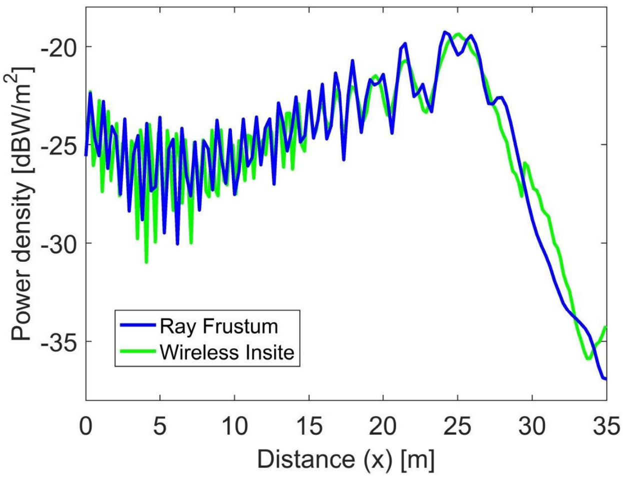

FIGURE 9. Comparison between the ray-frustum-based software and Wireless InSite (exposure limit - 10 dBW/m^2).

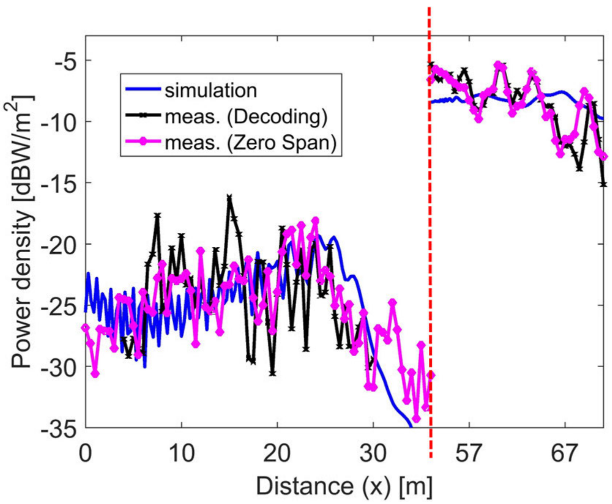

FIGURE 10. Measurement results of a 3.5 GHz 5G BS located in Daejeon, South Korea. Ray-tracing simulation is also shown for comparison (exposure limit - 10 dBW/m^2, $EIRP$ = 71.5 dBm).

path are shown in Figure 9. A good agreement between two results can be observed despite fairly small PD levels on the ground, which is attributed to a relatively high installation of a BS. The very low values of the PD relative to the 10 dBW/m^2 limit [40] is also clearly seen.

Figure 10 shows the measurement results of a 3.5 GHz 5G BS located in Daejeon, South Korea, obtained by two different methods of Decoding and Zero Span as discussed in Section II-B. It should be noted again that the measured data are scaled up based on the average value of the simulation results and the PDs are obtained based on the relation of $PD = \frac{E^2}{377}$ (i.e., the equivalent plane wave power density). Each marker in measured PD curves represents an actual measurement point with the spacing of $\Delta = 50$ cm. Note that the measurements along the ground path are only conducted over a distance less than 36 m since extremely low PD levels beyond this distance are hardly detectable. It is seen that the results of the Decoding method show slightly greater differences than those of the Zero Span method when compared with simulations. This is owing to the difficulty in detecting the accurate 5G SSB signals with low received powers at the ground level. Nonetheless, two measured PD behaviors show a good agreement with each other especially on the rooftop level, indicating that the proposed spacing of $\Delta = 1$ m can be very helpful for compliance measurements of a 5G BS. It is also observed that the overall trends of the scaled measurement results are also in agreement with those of the ray-tracings. The differences between measurements and simulations are mainly owing to the dynamic behavior of propagation environments (the BS specifications given in Table 1 may also be adjusted in the actual 5G wireless network in accordance with operating conditions). Note that all PDs are still do not exceed the exposure limit of 10 dBW/m^2 [40]. Also, it can be seen that the spacing of $\Delta = 1$ m can ensure four to five samples inside one crest of interference especially near the maximum distance, providing a good approximation to the overall PD profiles as a consequence. Therefore, it is evident that reasonable assessments can be conducted for installation compliances based on the $\Delta = 1$ m spacing, as discussed in detail above by using the two-ray propagation model. Note that although a fixed beam radiation is assumed for analysis to deduce the appropriate spacing of $\Delta = 1$ m, a beamforming scenario using multiple beams can be easily taken into account based on the superposition of all possible beams focusing different directions in the azimuth plane [14], [32].

IV. CONCLUSION

In this paper, a study on the appropriate measurement spacing used for installation compliance assessments of a 3.5 GHz 5G BS is presented. Ray-tracing simulations based on the ray frustum technique are conducted for three different installation scenarios on the elevation plane according to the accessibility categories from the ITU-T K.52 recommendation [29]. The simulation results from Scenario 1 indicate that the PD trends can be subdivided into three different regions with increasing the horizontal distance from a 5G BS. It can be seen that the farthest region (i.e., the "interference" region) has the most significant influence on an appropriate measurement spacing for reasonable EMF installation compliance assessments due to its interference pattern near the maximum distance. An interference analysis based on the two-ray propagation model indicates that the spacing of $\Delta = 1$ m for frequencies below 3 GHz can also be applied for 5G BS compliances up to 7.125 GHz, which is defined in the 3GPP specification [44] as the upper limit of FR1 for a 5G NR service. The overall PD trends in Scenarios 2 and 3, largely dependent on the relative installation height, indicate that the spacing of $\Delta = 1$ m established by simulations and analyses based on Scenario 1 can also be valid for the other installation scenarios having a significant reflecting structure near a BS. Validation of the $\Delta = 1$ m spacing from simulation studies is performed based on actual measurement of a 3.5 GHz 5G BS at a commercial site located in Daejeon, South Korea using two different NR extrapolation methods. The spacing of $\Delta = 1$ m proposed in this study will be incorporated into the standard for EMF installation compliances of a 5G BS in the future for effective measurement assessments.

ACKNOWLEDGMENT

(Young Seung Lee and Sang Bong Jeon contributed equally to this work.) The authors would like to thank Radio Environment and Convergence Business Division, Korea Radio Promotion Association, for their support and assistance during their measurements.

REFERENCES

[1] A. Ghosh, A. Maeder, M. Baker, and D. Chandramouli, "5G evolution: A view on 5G cellular technology beyond 3GPP release 15," *IEEE Access*, vol. 7, pp. 127639–127651, Sep. 2019.

[2] Reuters. *S.Korea First to Roll Out 5G Services, Beating U.S. and China*. Accessed: Feb. 2021. [Online]. Available: https://www.reuters.com/article/southkorea-5g/skorea-first-to-roll-out-5g-services-beating-us-and-china-idUSL3N21K114

[3] Korea Herald. *News Focus—Telecom Firms Plan to Commercialize Millimeter-Wave 5G Network*. Accessed: Feb. 2021. [Online]. Available: http://www.koreaherald.com/view.php?ud=20200420000849

[4] Korea Herald. *S.Korean 5G Subscribers Stand at Around 7m in Late May: Data*. Accessed: Feb. 2021. [Online]. Available: http://www.koreaherald.com/view.php?ud=20200609000171

[5] The Star. *Report: 5G Availability in S. Korea at Just 15%*. Accessed: Feb. 2021. [Online]. Available: https://www.thestar.com.my/tech/tech-news/2020/07/01/report-5g-availability-in-s-korea-at-just-15

[6] A.-K. Lee, S.-B. Jeon, and H.-D. Choi, "EMF levels in 5G new radio environment in Seoul, Korea," *IEEE Access*, vol. 9, pp. 19716–19722, Feb. 2021.

[7] *Effects of 5G Wireless Communication on Human Health*, Eur. Parliamentary Res. Service (EPRS) Briefing, Strasbourg, France, Mar. 2020.

[8] *Report Mobile Radio and Radiation*, Federal Dept. Environ., Transp., Energy Commun. (DETEC) Rep., Bern, Switzerland, Nov. 2019.

[9] M. Simkó and M. Mattsson, "5G wireless communication and health effects—A pragmatic review based on available studies regarding 6 to 100 GHz," *Int. J. Environ. Res. Public Health*, vol. 16, no. 18, p. 3406, Sep. 2019.

[10] S. Aerts, L. Verloock, M. Van Den Bossche, D. Colombi, L. Martens, C. Tornevik, and W. Joseph, "*In-situ* measurement methodology for the assessment of 5G NR massive MIMO base station exposure at sub-6 GHz frequencies," *IEEE Access*, vol. 7, pp. 184658–184667, Dec. 2019.

[11] D. Franci, S. Coltellacci, E. Grillo, S. Pavoncello, T. Aureli, R. Cintoli, and M. D. Migliore, "An experimental investigation on the impact of duplexing and beamforming techniques in field measurements of 5G signals," *Electronics*, vol. 9, no. 2, p. 223, Jan. 2020.

[12] D. Franci, S. Coltellacci, E. Grillo, S. Pavoncello, T. Aureli, R. Cintoli, and M. D. Migliore, "Experimental procedure for fifth generation (5G) electromagnetic field (EMF) measurement and maximum power extrapolation for human exposure assessment," *Environments*, vol. 7, no. 3, p. 22, Mar. 2020.

[13] S. Adda, T. Aureli, S. D'Elia, D. Franci, E. Grillo, M. D. Migliore, S. Pavoncello, F. Schettino, and R. Suman, "A theoretical and experimental investigation on the measurement of the electromagnetic field level radiated by 5G base stations," *IEEE Access*, vol. 8, pp. 101448–101463, May 2020.

[14] *Determination of RF Field Strength, Power Density and SAR in the Vicinity of Radiocommunication Base Stations for the Purpose of Evaluating Human Exposure*, Standard IEC 62232, Committee Draft, Ed. 3.0. Jun. 2020

[15] R. Yao, Y. Lu, T. Mekkawy, F. Xu, and X. Zuo, "Joint optimization of beamforming and power allocation for DAJ-based untrusted relay networks," *ETRI J.*, vol. 40, no. 6, pp. 714–725, Oct. 2018.

[16] *Basic Standard to Demonstrate The Compliance of Fixed Equipment for Radio Transmission (110 MHz–40 GHz) Intended for Use in Wireless Telecommunication Networks With the Basic Restrictions or the Reference Levels Related to General Public Exposure to Radio Frequency Electromagnetic Fields, When Put Into Service*, Standard EN 50400, CELENEC, Jun. 2006.

[17] B. C. Kim, H.-D. Choi, and S.-O. Park, "Methods of evaluating human exposure to electromagnetic fields radiated from operating base stations in Korea," *Bioelectromagnetics*, vol. 29, no. 7, pp. 579–582, Oct. 2008.

[18] *Notification for the Measurement of Electromagnetic Field Strength (Translated From the Original Korean Manuscript)*, Nat. Radio Res. Agency (RRA) Announcement 2019-3, Naju, South Korea, Mar. 2019.

[19] S.-C. Kim, B. J. Guarino, T. M. Willis, V. Erceg, S. J. Fortune, R. A. Valenzuela, L. W. Thomas, J. Ling, and J. D. Moore, "Radio propagation measurements and prediction using three-dimensional ray tracing in urban environments at 908 MHz and 1.9 GHz," *IEEE Trans. Veh. Technol.*, vol. 48, no. 3, pp. 931–946, May 1999.

[20] S. Hur, S. Baek, B. Kim, Y. Chang, A. F. Molisch, T. S. Rappaport, K. Haneda, and J. Park, "Proposal on millimeter-wave channel modeling for 5G cellular system," *IEEE J. Sel. Topics Signal Process.*, vol. 10, no. 3, pp. 454–469, Apr. 2016.

[21] F. Sheikh, Y. Gao, and T. Kaiser, "A study of diffuse scattering in massive MIMO channels at terahertz frequencies," *IEEE Trans. Antennas Propag.*, vol. 68, no. 2, pp. 997–1008, Feb. 2020.

[22] Y. S. Lee, H.-S. Lee, and H.-D. Choi, "A study on the convenient EMF compliance assessment for base station installations at a millimeter wave frequency," *J. Electromagn. Eng. Sci.*, vol. 18, no. 4, pp. 242–247, Oct. 2018.

[23] H. Kim and H.-S. Lee, "Accelerated three dimensional ray tracing techniques using ray frustums for wireless propagation models," *Prog. Electromagn. Res.*, vol. 96, pp. 21–36, Jan. 2009.

[24] C. Lauterbach, A. Chandak, and D. Manocha, "Interactive sound rendering in complex and dynamic scenes using frustum tracing," *IEEE Trans. Vis. Comput. Graphics*, vol. 13, no. 6, pp. 1672–1679, Nov. 2007.

[25] J. Tsakok, "Fast ray tracing techniques," M.S. thesis, Dept. Elect. Comput. Eng., Univ. Waterloo, Waterloo, ON, Canada, 2008.

[26] C. Kwon, H. Kim, H. Lee, H. H. Choi, W.-J. Byun, and K. Kim, "A temporal millimeter wave propagation model for tunnels using ray frustum techniques and FFT," *Int. J. Antennas Propag.*, vol. 2014, pp. 1–9, Apr. 2014.

[27] J. Lee, Y. Song, E. Choi, and J. Park, "MmWave cellular mobile communication for Giga Korea 5G project," in *Proc. 21st Asia–Pacific Conf. Commun. (APCC)*, Kyoto, Japan, Oct. 2015, pp. 179–183.

[28] B. Jeong, H. Kim, and H. Lee, "Indoor propagation of electromagnetic waves with orbital angular momentum at 5.8 GHz," *Int. J. Antennas Propag.*, vol. 2018, pp. 1–9, Jan. 2018.

[29] *Protection Against Interference; Guidance on Complying With Limits for Human Exposure to Electromagnetic Fields*, document ITU-T K. 52, Jan. 2018.

[30] F. Fontán and P. Espi neira, *Modeling the Wireless Propagation Channel—A Simulation Approach With MATLAB*, West Sussex, U.K.: Wiley, 2008.

[31] *Measurement of Radio Frequency Electromagnetic Fields to Determine Compliance With Human Exposure Limits When a Base Station is Put Into Service*, document ITU-T K.100, Jul. 2019.

[32] *Case Studies Supporting IEC 62232—Determination of RF Field Strength, Power Density and SAR in the Vicinity of Radiocommunication Base Stations for the Purpose of Evaluating Human Exposure*, Standard IEC TR 62669, Ed. 2.0. Apr. 2019.

[33] D. Colombi, P. Joshi, B. Xu, F. Ghasemifard, V. Narasaraju, and C. Törnevik, "Analysis of the actual power and EMF exposure from base stations in a commercial 5G network," *Appl. Sci.*, vol. 10, no. 15, p. 5280, Jul. 2020.

[34] *Study Channel Model for Frequencies From 0.5 to 100 GHz*, document 3GPP TR 38.901 V 16.1.0, Dec. 2019.

[35] D. He, B. Ai, K. Guan, L. Wang, Z. Zhong, and T. Kürner, "The design and applications of high-performance ray-tracing simulation platform for 5G and beyond wireless communications: A tutorial," *IEEE Commun. Surveys Tuts.*, vol. 21, no. 1, pp. 10–27, 1st Quart., 2019.

[36] A. Linhares, M. A. B. Terada, and A. J. M. Soares, "Estimating the location of maximum exposure to electromagnetic fields associated with a radiocommunication station," *J. Microw., Optoelectron. Electromagn. Appl.*, vol. 12, no. 1, pp. 141–157, Jun. 2013.

[37] P. E. Baltrenas and R. Buckus, "Measurements and analysis of the electromagnetic fields of mobile communication antennas," *Measurement*, vol. 46, no. 10, pp. 3942–3946, Dec. 2013.

[38] S. Jeon, A.-K. Lee, J. Um, and H.-D. Choi, "Estimation of EMF for base stations using signal decoding technique," in *Proc. URSI Asia–Pacific Radio Sci. Conf. (AP-RASC)*, New Delhi, India, Mar. 2019, pp. 179–183.

[39] P. E. Baltrenas, R. Buckus, and S. Vasarevičius, ''Research and evaluation of the intensity parameters of electromagnetic fields produced by mobile communication antennas,'' *J. Environ. Eng. Landscape*, vol. 20, no. 4, pp. 273–284, Nov. 2012.
[40] International Commission on Non-Ionizing Radiation Protection, ''Guidelines for limiting exposure to electromagnetic fields (100 kHz to 300 GHz),'' *Health Phys.*, vol. 118, no. 5, pp. 483–524, May 2020.
[41] D. Halliday, R. Resnick, and J. Walker, *Fundamentals of Physics*, 10th ed. Hoboken, NJ, USA: Wiley, 2014.
[42] C. Balanis, *Antenna Theory: Analysis and Design*, 3rd ed. Hoboken, NJ, USA: Wiley, 2005.
[43] S. Salous, *Radio Propagation Measurement and Channel Modelling*. West Sussex, U.K.: Wiley, 2013.
[44] *Base Station Radio Transmission and Reception*, document 3GPP TS 38.104 V 17.0.0, Dec. 2020.

YOUNG SEUNG LEE (Member, IEEE) received the B.S. degree in radio communications engineering from Korea University, Seoul, Republic of Korea, in 2006, and the M.S. and Ph.D. degrees in electrical engineering from the Korea Advanced Institute of Science and Technology, Daejeon, Republic of Korea, in 2008 and 2012, respectively. Since 2012, he has been with the Electronics and Telecommunications Research Institute, Daejeon, where he is currently a Senior Researcher. His current research interests include exposure system design, compliance assessment, and numerical dosimetry, with an emphasis on 5G and millimeter-wave frequencies. He is also concerned with electromagnetic theory and antenna propagation.

SANG BONG JEON received the B.S., M.S., and Ph.D. degrees in electronic engineering from Yeungnam University, Gyeongsan, Republic of Korea, in 2001, 2003, and 2007, respectively. From 2008 to 2010, he was a Senior Research Engineer with the Korea Radio Promotion Association, Seoul, Republic of Korea, where he conducted research in the fields of electromagnetic compatibility technology. Since 2010, he has been with the Radio and Satellite Research Division, Electronics and Telecommunications Research Institute, Daejeon, Republic of Korea. His research interests include bioelectromagnetics and electromagnetic compatibility.

AE-KYOUNG LEE received the B.S. and M.S. degrees in electronics and engineering from Chungang University, Seoul, Republic of Korea, in 1990 and 1992, respectively, and the Ph.D. degree in radio science and engineering from Chungnam National University, Daejeon, Republic of Korea, in 2003. In 1992, she joined the Radio Technology Group, Electronics and Telecommunications Research Institute, Daejeon, where she has been involved in projects on measurement technologies and numerical analyses of electromagnetic compatibility and human exposure to RF fields. She was a recipient of the Japan Microwave Prize at the 1998 Asia–Pacific Microwave Conference, Japan, and the Technology Award from the Korea Electromagnetic Engineering Society, in 1999.

KIHWEA KIM received the B.S. and M.S. degrees in physics from Sungkyunkwan University, Seoul, South Korea, in 1995 and 1997, respectively, and the Ph.D. degree in electrical and electronics engineering from Dankook University, Seoul, in 2016. Since 1997, he has been working with the National Radio Research Agency, Ministry of Science and ICT. His current research interests include electromagnetic field measurements from mobile devices and electric field strength in relation to the biological effect or human safety.

JEONG-KI PACK received the B.S. degree in electronic engineering from Seoul National University, Seoul, South Korea, in 1978, and the M.S. and Ph.D. degrees in electromagnetic wave propagation from Virginia Tech, USA, in 1985 and 1988, respectively. He joined ETRI, in 1988, and moved to Dona-A University, in 1989. From 1978 to 1983, he has worked with the Agency for Defence Development, South Korea, as a Researcher. Since February 1995, he has been a Professor with the Department of Radio Science and Engineering, Chungnam National University, Daejeon, South Korea, where he is currently an Emeritus Professor. His research interests include electromagnetic wave propagation and bioelectromagnetics.

HYUNG-DO CHOI received the M.S. and Ph.D. degrees in material sciences from Korea University, Seoul, Republic of Korea, in 1989 and 1996, respectively. Since 1997, he has been with the Electronics and Telecommunications Research Institute, Daejeon, Republic of Korea, where he is currently the Project Leader of the Radio and Satellite Research Division. He researched in the field of biological effects of RF radiation and developed RF radiation protection standards.